Label-free Optical Antibody Testing Kit Based on a Self-assemble Whispering-gallery-mode Microsphere

Ying Yue, Hui Ding,* and Chen Chen

The appearance of antibodies in blood is a critical signal to suggest the infection. A rapid and accurate detection method for the antibody is significant to the disease diagnosis, especially for the epidemic. To this end, a highly sensitive whispering-gallery-mode (WGM) optical testing kit is designed and fabricated for detecting the specific immunoglobulin antibodies. The key component of the kit is a silica self-assembled microsphere decorated with the nucleocapsid proteins (N-proteins) of the SARS-CoV-2 virus. After the N-protein antibody immunoglobulin G (N-IgG) and immunoglobulin M (N-IgM) solutions being injected into the kit, the WGM red-shifts due to the antigen-antibody reaction. The wavelength displacement rates are proportional to the concentrations of these two antibodies from 1 μg/ml to 100 μg/ml. A good specificity of the kit was demonstrated by the non-specific human immunoglobulin G (H-IgG) and immunoglobulin M (H-IgM).

1 Introduction

Rapid and accurate detection of the biomolecules is of huge significance for the fields of diagnosis, food safety, and environmental pollution.[1–4] Especially, the biosensors meet the urgent needs under the outbreak of the epidemic that affects a much great number of people all over the world. In the immune process, the antigens can induce the immune system to produce corresponding antibodies, and these antibodies have specific combinations to the antigens. The antigen-antibody reaction has been widely accepted in the serological ascertainment of exposure to infectious agents.[5] Compared with the primary method for viral RNA by methods such as RT-qPCR (quantitative reverse transcription PCR), antibody assay has several technical advantages. (i) Antibodies exist in the serum, which can be easily obtained by the standard blood collection. (ii) Antibody detection technique, for example the colloidal gold testing kit, does not require professional equipment and can be adopted in most of the hospitals and clinics.[6] (iii) Different types and concentrations of the antibodies reflect the course of disease, which helps the doctors to adjust the therapeutic plans.[7,8] (iv) The cost-effective and rapid detection process are beneficial to the large-scale screening in the train stations, airports and harbors. There has developed three typical strategies for antibody detection: immune colloidal gold technique (GICT),[9] Enzyme-linked immunosorbent assay (ELISA),[10] and chemiluminescence immunoassay (CLIA).[11] Unfortunately, all of them have to label biomarkers such as gold nanoparticles, isotopes, and fluorescent molecules on the reactants. This operation not only requires the complicated labeling steps but also consumes a lot of expensive biomarkers.

WGM microresonator has been used as an optical sensor in fundamental researches and practical applications. Owing to the high quality factor (Q factor) and small mode volume, it has high sensitivity to temperature,[12] pressure,[13] gas[14] and biomolecular objects such as protein,[15,16] nuclear acid,[17] antigen or antibody,[18,19] and virus.[20] However, the small surface area of these WGM components and the low power of their evanescent wave are the main reasons for their limited sensitivity. For example, the saturated wavelength displacement of the biosensor reported by D.-X. Xu[19] is 1.2 nm due to the limited binding sites. Moreover, the WGM biosensor, as an advanced label-free detection method for antibody, has barely been used for the specific antibodies detection yet.

In this letter, we design a label-free optical testing kit for antibody detection with a high sensitivity and specificity. The key component is a self-assembled silica mesoporous microsphere. It not only supports photonic WGM resonance but also has a large surface area with a great number of binding sites to allow numerous receptors conjugating. The mesopores allow the analytes infiltrating in to increase the overlapping of the light and analytes. The nucleocapsid protein, as known as N-protein, is one of the most important proteins on the SARS-CoV-2 virus since it participates in RNA package and virus particle release.[21] Accordingly, it can act as the specific receptors of the rapid diagnostic tool in immunology for the corresponding antibodies. We firstly study the sensitivity of the microsphere to the refractive index of the surrounding liquid media. Secondly, the responses of the kits to the N-IgG and N-IgM antibodies are examined and the prin-

School of Electrical Engineering, Xi'an Jiaotong University, 28 Xianning West Road, Xi'an City, Shaanxi Province 710049, China; E-mail: dinghui@mail.xjtu.edu.cn

† Electronic Supplementary Information (ESI) available: [details of any supplementary information available should be included here]. See DOI: 00.0000/00000000.

This article has been accepted for publication and undergone full peer review but has not been through the copyediting, typesetting, pagination and proofreading process which may lead to differences between this version and the Version of Record. Please cite this article as doi: 10.1002/jbio.202000338

ciple of the antigen-antibody reaction is analyzed. At last, the non-specific H-IgG and H-IgM as the control groups, are applied to the sensors to examine the specificity of the designed optical testing kit.

2 Methods

2.1 Preparation of the self-assembled microsphere

The fabrication method of the self-assembled microsphere and the related physical mechanism were introduced and discussed in our previous paper.[22] In brief, the silica nanoparticles with a diameter of ∼20 nm were dispersed in water with a concentration of 40 wt% and trace OH^- was added to avoid them aggregation (purchased from Ivkeyan). There were abundant hydroxyl groups on the surface of silica nanoparticles to both keep good hydrophilicity and generate strong electrostatic repulsion among the nanoparticles. A droplet of the dispersion with a volume of ∼0.1 μl was posited on an artificial superhydrophobic layer with a contact angle of ∼153° (prepared by the superhydrophobic granules deposition on a glass slide). Such a high contact angle helped the droplet to keep spherical shape throughout the self-assmebly process. After the dispersant evaporating, a silica microsphere with radius of ∼100 μm was formed.

2.2 Silanization of the microsphere

Silanization had been widely used to generate silane groups, and they were the bridges to connect the biomolecules and the hydroxyl groups on the inorganic materials. To modify the silane groups on the silica microsphere, 5% APTES (3-aminopropyltriethoxysilane) solution in ethanol solution was applied the microsphere at 50 °C for 3 h. In this process, siloxane bonds linked to the hydroxyl groups on the surface of the silica nanoparticles. After this operation, there were abundant amino groups on the silica nanoparticles. Subsequently, the microsphere was rinsed with deionized water (DI-water) for three times to remove the residual solution and any weakly coupled silane groups. It was then heated at 120 °C for 20 min to strengthen the bond energy between the silane groups and the microsphere. The microsphere was used immediately for antigen decoration.

2.3 Antigen conjugation on the microsphere

Commercially available SARS-CoV-2 coronavirus nucleocapsid proteins (N-proteins, SL-CON03, Hangzhou Sonice Biotechnology Co., Ltd), as the specific target receptors, were dissolved in 1× phosphate buffered saline (PBS, with the concentration of 10 mM, PH=7.4) solution with a concentration of 100 μg/ml. The silanized microspheres were incubated in the solution at 27 °C for 30 min to bind the N-proteins to the amino groups on the silica nanoparticles. The bonding was a silane coupling interaction. Then, the microsphere was rinsed entirely with DI-water to remove the weakly conjugated antigen molecules on the surface of the microsphere and dried with the air purging. The interaction between silica nanoparticles was Van de Waals force with active range of about 0.3-0.5 nm, so the gap between nanoparticles did not allow the big biomolecules infiltrated in and affect the interaction between them. The entire fabricating processes of the antigen decorated self-assembled microsphere were shown in Figure 1.

2.4 Design of the testing kit

The PMMA substrate with a size of 25 mm×35 mm×3 mm had a testing channel on its top surface with depth and width of 1 mm respectively. The channel was treated with the hydrophilic reagent (mesophilic-2000, purchase from MesoBioSystem) for 1 min to help the aqueous samples flowing smoothly. Then, silica gel was coated in the middle section of the channel to form a thin film with thickness of ∼1 μm. The gel was hydrophobic, so its coating area should be controlled to about 100 μm×100 μm to avoid the hydrophobicity affecting the liquid sample flowing. This silica gel had a strong adhesion to the microsphere to fix it in the specific location. Subsequently, a tapered fiber was prepared by fusing and stretching a single-mode fiber under an oxyhydrogen flame. The diameter of the fiber waist was ∼0.8 μm (measured by SEM) to provide both a strong evanescent field and a matched propagation constant between the fiber and the microsphere. After the distance between the fiber waist and the microsphere was precisely controlled to generate a resonant spectrum, each side of the fiber waist were fixed by an epoxy resin (Ergo 7300).

2.5 Measurement system

After the testing kit was connected to a SLED source (central wavelength λ=1534 nm, FWHM = 32nm) and an optical spectrum analyzer (OSA, Yokogawa, Q6370B), the resonance spectrum was generated. Commercially available SARS-CoV-2 coronavirus N-protein monoclonal humanized antibody immunoglobulin G (N-IgG, SL-CON-IgG, Hangzhou Sonice Biotechnology Co., Ltd) and SARS-CoV-2 coronavirus N-protein monoclonal humanized antibody immunoglobulin M (N-IgM, SL-CON-IgM, Hangzhou Sonice Biotechnology Co., Ltd) were dissolved in PBS with different concentrations from 0.5 μg/ml to 100 μg/ml. The PBS solution was initially injected into the testing channel and immersed the microsphere. Subsequently, one antibody sample was applied in the testing kit via an injector with a flow rate of ∼20 μl/s and volume of ∼20 μl. After the antibody samples were injected into the kit, the timer started from 0 and the transmitted spectrum was recorded every 30 s in the detection processes. Because of the immune complex was formed and attached on the microsphere, the testing kit is disposible. So, every testing should be applied to a new testing kit. Moreover, the commercially available human immunoglobulin G (H-IgG, Dingguo Biotechnology Co., Ltd) and human immunoglobulin M (H-IgM, Beijing Bersee Biotechnology Co., Ltd) with a concentration of 100 μg/ml in PBS solution, as the control groups, were applied in the testing kits as well.

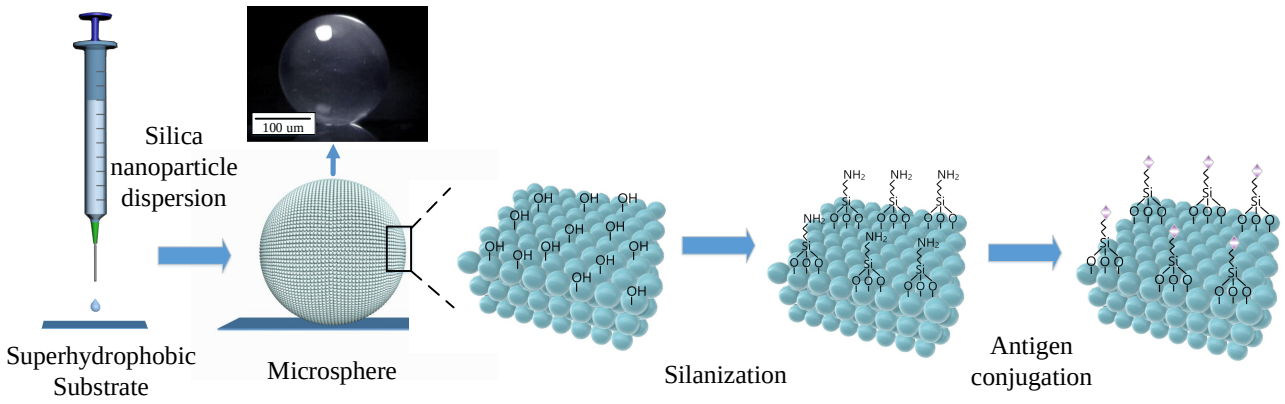

Fig. 1 The fabrication procedures of the self-assembled microsphere decorated with the antigen biomolecules. The micrograph is the silica nanoparticles self-assembled microsphere with radius of ~100 μm.

3 Result and Discussion

3.1 The sensitivity of the self-assembled microsphere to the surroundings

In the photonic WGM, the resonant wavelength λ of the transmitted spectrum can be expressed as:

$$\lambda = \frac{2\pi R n_{eff}}{m} \tag{1}$$

where R is the radius of the self-assembled microsphere, n_{eff} is the effective refractive index of the optical path, and m is the resonant order. When the host media is air with the refractive index of ~1.000, almost all of energy is confined in the microsphere and n_{eff} approximates to the refractive index n_s of the microsphere. In the case of liquid material as the host media, more proportion of the photonic energy leaks into the host media, and n_{eff} is actually determined by both n_s and the refractive index n_h of the host media.

According to the analysis of the WGM,[23] the resonant wavelength displacement can be expressed as:

$$\frac{\Delta\lambda}{\lambda} = \frac{\Delta n_h}{n_h} F + \frac{\Delta n_s}{n_s}(1-F) + \frac{\Delta R}{R} \tag{2}$$

where, F is a sensitivity coefficient related to the special distribution of the light power at the microsphere surface. From Equation (2), the resonant wavelength will red-shift with the enlargement of the microsphere size, increases of the refractive indexes of microsphere and host media respectively.

Based on the nanoparticles self-assembly structures,[24] the nanoparticles in the microsphere tend to arrange as a hexagonal close-packed structure or face-centered cubic structure with filling factor of 0.74. Based on the effective medium theory, the refractive index n_s of the microsphere can be approximately expressed as

$$n_s = \sqrt{0.74 n_p^2 + 0.26 n_h^2} \tag{3}$$

where, n_h is the refractive index of the host media, and n_p=1.475 is the refractive index of individual silica nanoparticles as reported by Khlebstov.[25] From Equation (3), it can be deduced that n_s increases with n_h, as shown as Figure 2a. This character of the self-assembled microsphere is much different from the typical fused silica microsphere whose refractive index is constant.

Experimentally, the self-assembled microsphere fabricated by the procedure 1 in Methods was installed in the testing kit and connected to the measurement system by the procedure 4 and 5, as shown in Figure 2b. In the different host media of air (n=1.000), DI-water (n=1.3330), and PBS (n=1.3338), the resonant spectra of the self-assembled microsphere were shown in Figure 2c. In the liquid media, both the transmitted intensity and the resonant depth of the spectra decreased because of more photons leaking into the surroundings. The Q factor of the microsphere in the aqueous solution was ~1000. By monitoring a resonant peak, the WGM was found to rad-shift ~0.40 nm after the host media changed from DI-water to PBS solution. Hence the sensitivity of the self-assembled microsphere to the liquid media can be calculated to

$$\delta = \frac{0.4nm}{1.3338 - 1.3330} = 500nm/RIU \tag{4}$$

Due to the resolution of the OSA is 20 pm, the self-assembled microsphere has a resolution as high as $4\times10^{-5}RIU$ to the surroundings.

Such high sensitivity and resolution are critical for detecting the trace analytes with low concentration in solutions. So, a more accurate experiment was carried out, A solution with 5% PBS solution and 95% deionized water was prepared. The refractive index of this solution was calculated to be 1.33304 accroding to the effective media theory. DI-water and such solution were used to test the resonant spectrum shifting with the experimental result shown in Figure 2d. In the experimental result, the limitation of detection of the self-assembled sensor to the refractive index was $4\times10^{-5}RIU$, which accordance with the calculated value.

Sensitivity is determined by the interaction between light in the device and the matter to be measured. This interaction include the spatial and temporal domains. Researchers tend to pursuit a higher Q factor to lengthen the interaction time of light and the objects. Therefore, their WGM sensors have a high sensitivity.

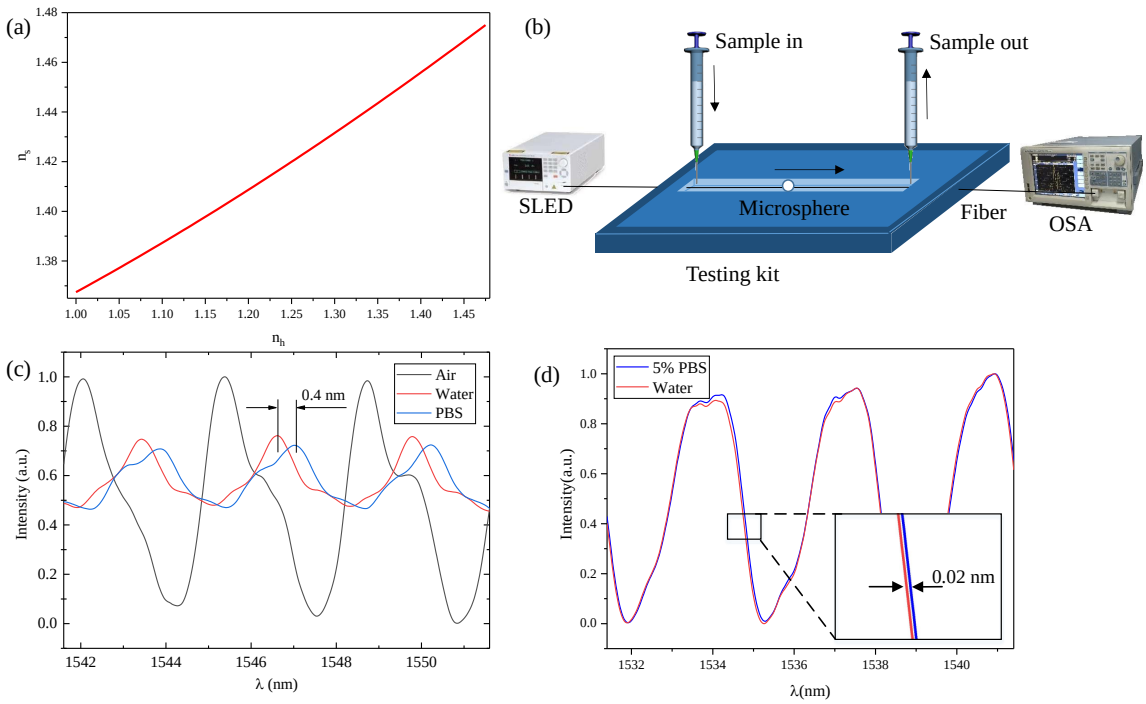

Fig. 2 Response of the silica self-assembled microsphere to different host medium. (a) The n_s versus n_h by Equation 3. (b) Schematic of the measurement system setup. (c) The resonant spectra of the self-assembled microsphere in the host medium of air, water and PBS respectively. (d) The resonant spectra of the microsphere in the host medium of water and 5% PBS solution.

However, those devices universally use evanescent filed to sense the host media, which means only a small part of light energy in space interacting with the analytes. Different from them, the self-assembled microsphere finds a new way to strengthen the light-matter interactions, who has mesoporous structures to enable the object infiltrated in the microsphere, and this will dramatically increase the overlapping between the light and object spatially. Furthermore, the porous property of the self-assembled microsphere promotes the sensitivity of the WGM devices to the surroundings although the Q factor is not very high.

3.2 The response of the testing kit to the specific antibodies: N-IgG and N-IgM

As well known, the antibody biomolecules disperse uniformly in the aqueous solution because the superficial polar groups induce strong hydrophilicity. Also, the polar groups generate strong electrostatic repulsion among the biomolecules to avoid them aggregating. Each molecule of the antibody has two identical binding sites. The specificity of an antibody for an antigen depends entirely upon the possession of the appropriate epitope by an antigen. Each binding site on the antibody and each epitope on the antigen are complementary regions on the surface of the respective molecules which interlock in the antigen-antibody reaction. The interactions between them are noncovalent bonds, including Van der Waals force, electrostatic force, hydrogen bond, and hydrophobic interaction.[26] Once the antigen decorated microsphere is immersed into the specific antibody solutions, the antibody

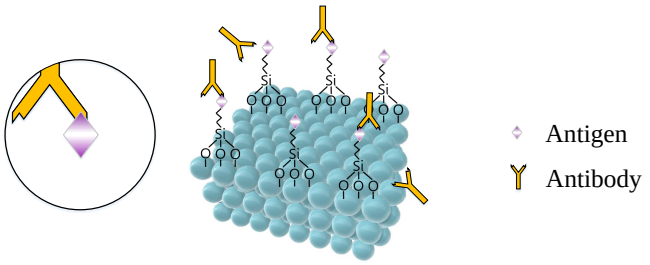

Fig. 3 The capture of the antibody in solution by the antigen on the surface of the self-assembled microsphere in the antigen-antibody reaction. The close-up diagram shows the complementary characters of the antibody binding site and the antigen epitope.

biomolecules are captured by the antigen epitopes to produce immune complexes as show in Figure 3. The immune complex consists of closely apposed but still discrete molecules of antigen and antibody. Owing to the binding actions, the surface characteristics of both the antibody and antigen are changed and the immune complexes tend to become hydrophobic. Subsequently, the agglutination and precipitation of the immune complexes occur on the surface of the silica microsphere. Immune complexes comprising many molecules eventually enlarge the radius and change the effective refractive index on the surface of the self-assembled microsphere.

In the experiment, the N-protein decorated self-assembled microsphere was installed into the testing kit and connected to the

measurement system, which was the same as that in Figure 2b. According to the research results form Ma, etc.[8], we obtained the accurate values about the specific antibody concentration in blood of patients: N-IgM concentration reaches its peak of 7.25 μg/ml about 11-15 days after illness onset; and N-IgG concentration reaches its peak of 16.47 μg/ml about 21-25 days after illness onset and stays at a high concentration of 11.4 μg/ml for a long-time. The relationship between the wavelength displacement and the time were shown in Figure 4 at different concentrations of N-IgG and N-IgM solutions. The response of the testing kit to the pure PBS solution with antibody concentration of zero was also presented as the reference.

In Figure 4a, the displacements of the resonant wavelength were 2.24 nm, 0.9 nm and 0.22 nm respectively when the N-IgG solutions were applied to the kit for 1500 s with concentrations of 100 μg/ml, 10 μg/ml and 1 μg/ml respectively. The response curves of the kit to the N-IgG solutions showed linear growing rate, which was much different from that to the pure PBS solution. Moreover, the higher of the antibody concentration, the earlier of the resonant spectrum began to shift. The result of wavelength shifting was determined by the proportion of the antigen and antibody. If the binding sites on the antibody was equal to the epitopes on the antigen, the optimal ratio was achieved and abundant immune complex were produced. The wavelength displacements illustrated that the concentration of 100 μg/ml was closer to the optimal ratio, and the concentrations of 10 μg/ml and 1 μg/ml were in the post-zone of the immune reaction with too few antibody biomolecules taking part in the reactions. The antigen-antibody reaction had a positive effect on the raise of the radius of the microsphere and/or the effective refractive index on the surface of the microsphere.

In Figure 4b, the response curves showed step-like rising trends, which were different from the straight lines of N-IgG. This difference were beneficial to helping the analysts to distinguish the antibody types. In the immune system, the IgM was a type of early antibody that suggested the primary infection, while the IgG was a product of the secondary immune response that suggested the body entering the recovery period or having a past infection. The displacements of the resonant wavelength were 1.58 nm, 0.58 nm and 0.1 nm respectively when the N-IgM samples with concentrations of 100 μg/ml, 10 μg/ml and 1 μg/ml were applied to the kit for 1500 s. Among these curves, the blue one showed no obvious difference from the reference line, which demonstrated that 1 μg/ml of N-IgM was lower than the limitation of detection of the biosensor. Moreover, a rapid rise of wavelengths at 0 s was caused by the refractive index changing of the host media due to the injection of antibody solution.

Taking the N-IgG solution with concentration of 100 μg/ml as an example, the dynamic spectrum movement of the biosensor was shown in Figure 4c. The WGM resonant wavelength kept red-shift once the N-IgG solution was injected into the testing kit and the shifting rate was constant. Accordingly, the spectrum shifting rate $\triangle\lambda/\triangle$t was analyzed at different concentration for two kinds of specific antibodies. As shown in Figure 4d, it was found that the shifting rate increased with the concentration of the antibodies for both the two antibodies. Each error bar came from the three independent measurements of the antibodies. Moreover, at the same concentration, the shifting rate for N-IgG was little larger than that for N-IgM. The higher sensitivity of the kit to the N-IgG than N-IgM may be caused by the different structures and refractive indexes of two immune complexes respectively. The dynamic detection range (1 μg/ml-100 μg/ml) of the biosensor satisfied the detection of the antibody in the patient and accomplished the disease diagnosis. To ensure the response signal is much different from the reference line. The limitations of detection are defined as 1 μg/ml and 2 μg/ml for the N-IgG and N-IgM respectively.

The calibration curve for N-IgG antibody in the concentration range of 0.5-20 ug/ml can be expressed as:

$$\frac{\Delta\lambda}{\Delta t} = 0.00245C + 0.00712 \tag{5}$$

where C is the concentration of the antibody. While, for N-IgM with concentration varying from 1 to 10 ug/ml, the relation can be expressed as

$$\frac{\Delta\lambda}{\Delta t} = 0.00217C + 0.00334 \tag{6}$$

According to the Equation (1) and (2), we conclude that the refractive of the microsphere maybe enlarged due to the capture of the antibody by the antigen on the surface of the self-assembled microsphere. At the same time, due to the formation of the antigen-antibody composite, the radius of the microsphere maybe also enlarged which has positive effect to the wavelength red-shift as well.

3.3 The response of the testing kit to the non-specific antibody: H-IgG and H-IgM

In order to weigh the specificity of the antigen decorated kit to the antibodies, the human immunoglobulin G (H-IgG) and human immunoglobulin M (H-IgM) were examined by the optical testing kit. In the experiment, the H-IgG and H-IgM solutions with a highest concentration of 100 μg/ml were injected into the testing kit respectively. The response curves oscillated with maximum wavelength shift of $\sim$0.1 nm and $\sim$0.12 nm respectively, as shown in Figure 5. A sharp raising of the green line at 0 s resulted from the refractive index changing once the antibody solution being injected in the kit. These curves were relatively flat with little changing in the wavelength displacement, which were similar to the reference line (response of the kit to PBS solution), and much different from those caused by N-IgM and N-IgG with the same concentration. Because they were not the immune response products against the SARS-Cov-2 virus, the commercially available H-IgG and H-IgM samples do not have the specific binding sites for the N-protein epitope. Thereby, different from the specific antibodies of N-IgG and N-IgM, they cannot interlock with the N-protein on the self-assembled microsphere.

Therefore, it can be concluded that the red-shifts of the WGM resonant wavelength in Figure 4a and 4b were mainly caused by the binding action of antibody biomolecules on the microsphere by the antigen-antibody reaction. It also demonstrated that the designed testing kit has a good specificity since the wavelength

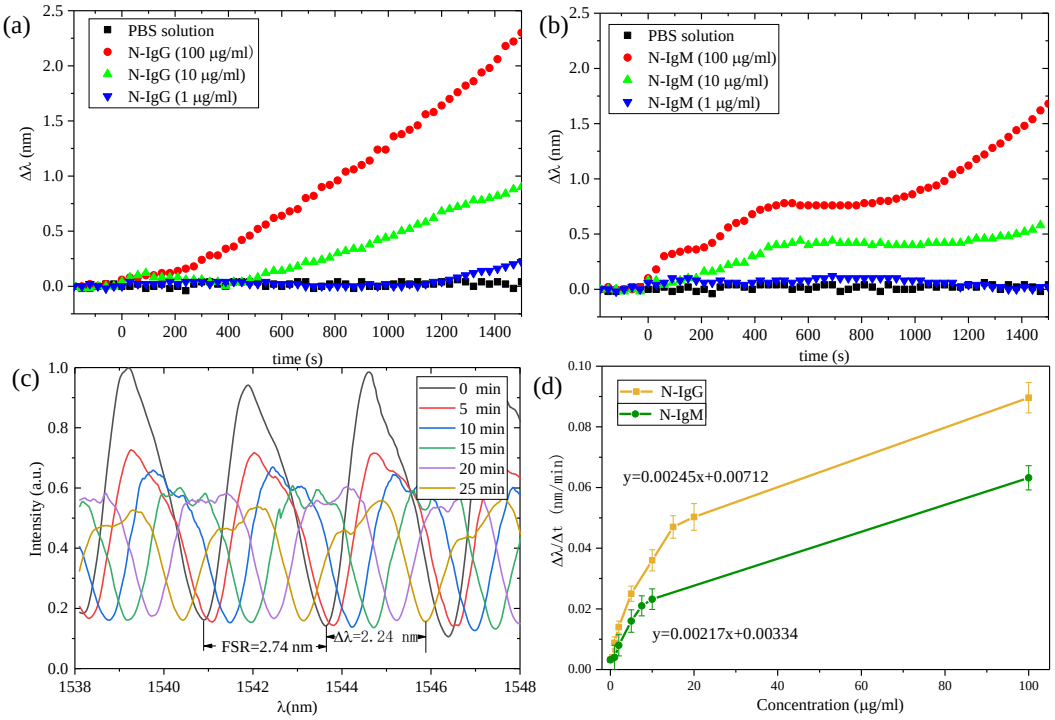

Fig. 4 Wavelength responses of the optical kit to the specific antibodies. (a) Wavelength displacement versus time at different N-IgG concentrations from 1 μg/ml to 100 μg/ml. The response of the kit to PBS solution was shown as the reference. (b) Wavelength displacement versus time at different N-IgM concentrations from 1 μg/ml to 100 μg/ml. (c) The dynamic spectrum movement of the biosensor to the N-IgG with concentration 100 μg/ml. (d) The spectrum shifting rate of biosensor at different concentrations for N-IgG and N-IgM antibodies respectively.

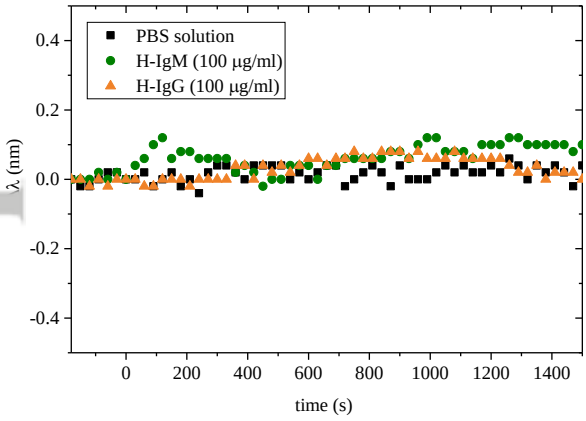

Fig. 5 Wavelength displacements of the optical kit to the H-IgG and H-IgM solutions with concentration of 100 μg/ml. The response of the kit to PBS solution was shown as the reference.

signal responding only to the N-IgG and N-IgM antibodies. This result revealed the huge application potential of this optical kit to accurately distinguish the patients of the SARS-CoV-2 coronavirus infection and the healthy people.

4 Conclusion

The key component of the designed optical testing kit for antibody detection is the self-assembled silica microsphere with a high sensitivity of 500 nm/RIU to the refractive index of the host media. It not only allows the photonic WGM resonance to strengthen the light-matter interaction in spatial domain but also provides a large surface area to capture more objective analytes. Taking the N-protein of the SARS-CoV-2 virus as the receptors, the antigen decorated microsphere had a high sensitivity to the specific N-IgG and N-IgM antibody biomolecules. Although the testing kit is disposable, thanks to the small volume of the sensing device in the testing kit, this sensor has a relative low cost for about 2-3 US dollar. In the future work, we expect to further reduce the size of the self-assembled microsphere to match the width of the microfluidics channels. By this way, a microsphere embedded microfluidics system will accomplish a complex blood assay in one step. Thereby. the self-assembled WGM microsphere decorated with antigens will have huge potential for the applications of clinical diagnosis and laboratory researches.

Conflicts of interest

There are no conflicts to declare.

Acknowledgements

National Natural Science Foundation of China (NSFC) (51777150).

Notes and references

1 B. Bohunicky and S. A. Mousa, *Nanotechnology, Science and Applications*, 2010, **4**, 1–10.

2 A. Amine, H. Mohammadi, I. Bourais and G. Palleschi, *Biosensors Bioelectronics*, 2006, **21**, 1405–1423.

3 B. V. Dorst, J. Mehta, K. Bekaert, E. Rouah-Martin, W. D. Coen, P. Dubruel, R. Blust and J. Robbens, *Biosensors Bioelectronics*, 2010, **26**, 1178–1194.

4 K. R. Rogers, *Analytica Chimica Acta*, 2006, **568**, 222–231.

5 S. Hashida, K. Hashinaka, S. Ishikawa and E. Ishikawa, *Journal of Clinical Laboratory Analysis*, 267–286.

6 Z. Li, Y. Yi, X. Luo, N. Xiong and F. Ye, *Journal of Medical Virology*, 2020.

7 A. Sa-Ngasang, S. Anantapreecha, A. A-Nuegoonpipat, S. Chanama, S. Wibulwattanakij, K. Pattanakul, P. Sawanpanyalert and I. Kurane, *Epidemiol. Infect.*, 2006.

8 H. Ma, W. Zeng, H. He, D. Zhao, Y. Yang, D. Jiang, P. Zhou, Y. Qi, W. He, C. Zhao, R. Yi, X. Wang, B. Wang, Y. Xu, Y. Yang, A. J. Kombe Kombe, C. Ding, J. Xie, Y. Gao, L. Cheng, Y. Li, X. Ma and T. Jin, 2020.

9 X. Sun, X. Zhao, T. Jian, J. Zhou and F. S. Chu, *International Journal of Food Microbiology*, 2005, **99**, 185–194.

10 M. R. Salimi-Bejestani, J. W. Mcgarry, S. Felstead, P. Ortiz, A. Akca and D. J. L. Williams, *Research in Veterinary Science*, 2005, **78**, 0–181.

11 D. D. Robert, T. Mageli, M. D. A. Fernandez and H. Barbara, *Clinical Chemistry*, 2020, 6.

12 C. H. Dong, L. He, Y. Xiao, V. R. Gaddam, S. K. Ozdemir, Z. F. Han, G. C. Guo and L. Yang, *Applied Physics Letters*, 2009, **94**, 231119.

13 R. Henze, T. Seifert, J. M. Ward and O. Benson, *Optics Letters*, 2011, **36**, 4536–4538.

14 V. D. Ta, R. Chen, D. M. Nguyen and H. Sun, *Applied Physics Letters*, 2013, **102**, 031107.

15 A. Yalcin, K. C. Popat, J. C. Aldridge, T. A. Desai, J. Hryniewicz, N. Chbouki, B. E. Little, O. King, V. Van and S. Chu, *IEEE Journal of Selected Topics in Quantum Electronics*, 2006, **12**, 148–155.

16 Y. J. Chen, W. Xiang, J. Klucken and F. Vollmer, *Nanotechnology*, 2016, **27**, 164001.

17 A. Ramachandran, S. Wang, J. Clarke, S. J. Ja, D. Goad, L. Wald, E. M. Flood, E. Knobbe, J. V. Hryniewicz and S. T. Chu, *Biosensors Bioelectronics*, 2008, **23**, 939–944.

18 T. Tajiri, S. Matsumoto, T. Imato, T. Okamoto and M. Haraguchi, *ieee sensors*, 2014, 641–644.

19 D. X. Xu, M. Vachon, A. Densmore, R. Ma and J. H. Schmid, *Optics Letters*, 2010, **35**, 2771–2773.

20 M. S. Mcclellan, L. L. Domier and R. C. Bailey, *Biosensors and Bioelectronics*, 2012, **31**, 388–392.

21 W. Zeng, G. Liu, H. Ma, D. Zhao and T. Jin, *Biochemical and Biophysical Research Communications*, 2020, **527**, year.

22 D. Hui, Y. Ying, C. Han and S. Chen, *Optics Letters*, 2018, **43**, 2619–.

23 G. Schweiger and M. Horn, *Journal of the Optical Society of America B Optical Physics*, 2006, **23**, págs. 212–217.

24 M. C. Goncalves, J. Bras and R. M. Almeida, *Journal of Sol-Gel Science and Technology*, 2007, **42**, 135–143.

25 B. N. Khlebtsov, V. Khanadeev and N. G. Khlebtsov, *Langmuir*, 2008, **24**, 8964–8970.

26 T. Osajima, M. Suzuki, S. Neya and T. Hoshino, *Journal of Molecular Graphics Modelling*, 2014, **53**, 128–139.